NEOPLASIA
www.neoplasia.com

Volume 21 Number 1 January 2019 pp. 106–116 106

Attenuation of Tumor Suppressive Function of FBXO16 Ubiquitin Ligase Activates Wnt Signaling In Glioblastoma[1]

Mohsina Khan[*], Dattatraya Muzumdar[†] and Anjali Shiras[*]

[*]National Centre for Cell Science (NCCS), SP Pune University Campus, Ganeshkhind, Pune, 411007, India; [†]Department of Neurosurgery, King Edward Memorial Hospital, Parel, Mumbai 400 012. India.

Abstract

Glioblastoma (GBM) is one of the most aggressive and lethal types of brain tumor. Despite the advancements in conventional or targeted therapies, median survival of GBM patients is less than 12 months. Amongst various signaling pathways aberrantly activated in glioma, active Wnt/β-catenin signaling pathway is one of the crucial oncogenic players. β-catenin, an important mediator of Wnt signaling pathway, gets phosphorylated by GSK3β complex. Phosphorylated β-catenin is specifically recognized by β-Trcp1, a F-box/WD40-repeat protein and with the help of Skp1 it plays a central role in recruiting phosphorylated β-catenin for degradation. In GBM, expression of β-TrCP1 and its affinity for β catenin is reported to be very low. Hence, we investigated whether any other members of the E3 ubiquitin ligase family could be involved in degradation of nuclear β-catenin. We here report that FBXO16, a component of SCF E3 ubiquitin ligase complex, is an interacting protein partner for β-catenin and mediates its degradation. Next, we show that FBXO16 functions as a tumor suppressor in GBM. Under normal growth conditions, FBXO16 proteasomally degrades β-catenin in a GSK-3β independent manner. Specifically, the C-terminal region of FBXO16 targets the nuclear β-catenin for degradation and inhibits TCF4/LEF1 dependent Wnt signaling pathway. The nuclear fraction of β-catenin undergoes K-48 linked poly-ubiquitination in presence of FBXO16. In summary, we show that due to low expression of FBXO16, the β-catenin is not targeted in glioma cells leading to its nuclear accumulation resulting in active Wnt signaling. Activated Wnt signaling potentiates the glioma cells toward a highly proliferative and malignant state.

Neoplasia (2019) 21, 106–116

Introduction

Gliomas are the most common and lethal tumors of the Central Nervous System (CNS) [1]. The grade IV glioma known as glioblastoma (GBM) is very fatal, with median survival of patients being only about 12–14 months [2]. GBM is considered to be driven by a subpopulation of cells known as "Glioma Stem Cells" (GSC) that perpetuate tumor growth and are considered to be responsible for therapy resistance [3]. Molecular events including mutations in IDH1 [4] and TP53 [5] genes, loss of heterozygosity (LOH) with 1p/19q co-deletion [6], loss of tumor suppressive miRNAs [7] and activation of oncogenic miRNAs [8] are some of the important mediators known to contribute to glioma initiation and progression.

Several developmental signaling pathways like Notch or Hedgehog pathways are shown to be deregulated in glioma [9–11]. Our earlier studies have reported the role of Wnt signaling pathway in glioma progression, wherein we have shown that an over activated Wnt

Abbreviations: GBM, Glioblastoma; LGG, Low-grade glioma; HGG, High-grade glioma; CNS, Central nervous system; GSC, Glioma stem-like cells; IDH, Isocitrate dehydrogenase; LOH, Loss of heterozygosity; WNT, Wingless-related integration; TCF, T-cell factor/lymphoid enhancer-binding factor; GSK-3β, Glycogen synthase kinase3-β; LEF, Lymphoid enhancer factor-1; SCF, Skp1, cullins, F-box proteins; NOD-SCID, Non-obese diabetic/severe combined immunodeficiency; IVIS, In vivo imaging system; PEI, Polyethyleneimine25000

Address all correspondence to: Anjali Shiras, National Centre for Cell Science (NCCS), SP Pune University Campus, Ganeshkhind, Pune, 411007, India.
E-mail: anjali@nccs.res.in

[1] Funding: This work was supported by funding from Department of Biotechnology, New Delhi, India, Cancer Biology Task Force, BT/PR10852 and intra-mural funding support from National Centre for Cell Science (NCCS) Pune, India. Fellowship support for MK was from University Grand Commission (UGC), New Delhi, India.
Received 1 November 2018; Revised 12 November 2018; Accepted 12 November 2018

1476-5586
https://doi.org/10.1016/j.neo.2018.11.005

signaling pathway mediated through stabilization of β-catenin is an important driver in propelling glioma progression and pathogenesis [12]. Several studies have extensively elaborated on mechanisms of active Wnt signaling in cancer and have shown that the deregulation is mediated mainly through the destruction complex- AXIN, APC, GSK-3β and β-TrCP1 [13]. Under normal conditions in the absence of a Wnt signal, this complex is constitutively active, phosphorylating specific residues in the N-terminus of β-catenin, leading to its ubiquitination and subsequent proteasomal degradation [14,15]. Later, the SCF-β-TrCP complex mediates destruction of cytoplasmic fraction of β-catenin [16,17]. The SKP1–Cullin–F-box protein (SCF) E3 ubiquitin ligase complex regulates multiple cellular processes through ubiquitination and subsequent degradation of target proteins.

To understand the mechanisms that lead to nuclear stabilization of β-catenin, we generated a model system comprising of a pair of cell lines derived from single GBM tumor tissue. Interestingly, the parental cell line was non-tumorigenic in nature, whereas the spontaneously emerged clones were highly proliferative and showed malignant phenotypes. Using this system of paired cell lines, we delineated the events responsible for nuclear β-catenin stabilization. Our studies have led to the functional annotation of a member of FBXO family of proteins, FBXO16 as a tumor suppressor that is downregulated in GBM in a graded manner. Next, we provide evidence of a specific interaction of FBXO16 with an important mediator of Wnt signaling pathway, β-catenin and prove the significance of this interaction to glioma progression. Our data demonstrate that under physiological conditions, FBXO16 effectively targets β-catenin for degradation and thereby maintains Wnt Signaling in an OFF state. In contrast, in GBM tumors where the FBXO16 levels are low, β-catenin is stabilized and retained in the nucleus leading to a hyperactivated Wnt signaling. In summary, we demonstrate the role of FBXO16 as a tumor suppressor and unequivocally establish deregulated Wnt signaling as a main driver for oncogenesis in GBM.

Materials and Methods

Tumor Tissues and Patient-Derived Tumor Cell Lines

The glioma and epileptic tissue resection samples were obtained from AFMC Hospital, Pune and KEM Hospital, Mumbai. The use of clinical specimens was approved by the Institutional Ethics Committees (IEC) of NCCS, AFMC Hospital; Pune and KEM Hospital, Mumbai, India. Classification of tumor tissues into various glioma grades was performed by a neuropathologist by following the WHO classification system [18]. The cell lines used in this study were established from tumor tissues (Supplementary Table 1) by following the methods described by us earlier [19,20].

RNA Extraction and Quantitative Real-Time PCR

The tissue samples were homogenized by using liquid nitrogen and total RNA was extracted using TRIzol Reagent (Invitrogen) using manufacturer's instructions. Quantitative RT-PCR (qRT-PCR) was performed using Power-up SYBR Green (Applied Biosystems, Carlsbad, CA) using QuantStudio 6 Flex Real-Time PCR system (Thermo-Scientific). Primer sequences used are listed in Supplementary Table 2.

Plasmids and Transient Transfections

The FBXO16 constructs viz.: FLAG-FBXO16 full length (WT), C-terminal deletion (ΔC), FBOX domain deletion (ΔF) and N-terminal deletion (ΔN) mutants were procured from Genscript; (Piscataway, NJ, USA). Three individual shRNAs to FBXO16 were designed using the RNAi Consortium shRNA library, BROAD institute, Cambridge, MA, and cloned into pLKO.1-TRC plasmid. The sequences of shRNAs designed for targeting FBXO16 transcripts were as follows:

sh1 sense - 5′GCTATTGAATGACCGGGTATTCTCGAGAA TACCCGGTCATTCAATAGC.
3′ antisense - 5′ GCTATTGAATGACCGGGTATTCTCGA GAATACCCGGTCATTCAATAGC 3′,
sh2 sense 5′ GATCTGGAAGAAGCACTATATCTCGAGA TATAGTGCTTCTTCCAGATC 3′,
antisense 5′ GATCTGGAAGAAGCACTATATCTC GAGATATAGTGCTTCTTCCAGATC 3′ and for.
sh3 sense 5′ CAAGCTTCCAAGGGTGTTATCCTCGAGGA TAACACCCTTGGAAGCTTG 3′,
antisense 5′ CAAGCTTCCAAGGGTGTTATCCTCGAGGA TAACACCCTTGGAAGCTTG 3′.

The sequences of Scrambled shRNA used as sh control were,

sense 5′ GCGATCGTAATCACCCGAGTGCTCGAGCA CTCGGGTGATTACGATCGC 3′,
antisense 5′ GCGATCGTAATCACCCGAGTGCTCGAGCA CTCGGGTGATTACGATCGC 3′.

The cells were transfected with Polyethyleneimine 25000 (PEI) following manufacturer's protocol [21]. Knockdown efficiencies of individual shRNA sequences were determined by using Western blotting (Supplementary Fig. 3).

Stable Cell Line Generation

To generate stable cell lines, control (RANG-2-EV) and FBXO16 overexpressing cells (RANG-2-FLAG-FBXO16) were selected with 750 μg/ml Geneticin (Sigma; San Diego, CA). Three independent clones over expressing FBXO16 were selected.

Western Blotting

Whole cell lysate proteins were prepared using M-per mammalian protein extraction reagent (Thermo Scientific, Waltham, MA, USA) with 1×protease inhibitor cocktail (Sigma) following manufacturer's instructions. Protein expression was detected using ECL-plus kit (Thermo Scientific).

Antibodies

SOX2 (Cat #3579), β-catenin (Cat #9562S & 9582S), FLAG (Cat # 9146S), ϒH2AX (Cat #9712S), H2AX (Cat #2595S) and K-48 (Cat # 8081) were purchased from Cell Signaling, Danvers, MA, USA. C-MYC (Cat # ab32072), Nestin (Cat # ab27952), Ki67 (Cat # ab16667) and Cyclin D1 (Cat # ab16663) were purchased from Abcam, Cambridge, MA, USA. Three individual antibodies to FBXO16 with Cat # NBP1–57614, AV53227 and PA566195 were procured from Novus Biologicals; Littleton, CO, USA, Sigma; St. Louis, Missouri, United States and Pierce; Waltham, MA, USA. The other antibodies used were Ub (Cat # Sc8017, Santa Cruz, Paso Robles, CA; USA), tubulin (Cat # T9026, Sigma) and actin (Cat # 691002, MP Biomedicals, CA, USA).

Immunoprecipitation

Immunoprecipitation was performed using total cell lysates using procedure described earlier [22]. Also, cells were fractionated into nuclear and cytoplasmic fractions. Briefly, the cell lysates were individually

immunoprecipitated overnight using antibodies to FBXO16, β-catenin or FLAG-tag. Antigen–antibody complexes were pulled-down using Dynabeads (Invitrogen) following manufacturer's instructions. Proteins were resolved on 10% SDS-PAGE gel and transferred onto PVDF membranes and detected using ECL-plus kit (Thermo Scientific).

Confocal Microscopy

Cells were seeded onto coverslips, transfected with pcDNA-3.1-FLAG (Control), FLAG-FBXO16 (Genscript; Piscataway, NJ) and RFP-β-catenin constructs using PEI. [21] Confocal imaging was performed using method described earlier [23]. For immunohistochemical analyses, tissue sections were deparaffinized by heating in microwave and washed with xylene and alcohol. This was followed by antigen retrieval and staining performed using method described earlier [24]. Images were acquired using Leica TCS SP5II (Leica Microsystems CMS, GmbH, Germany) confocal microscope.

Ubiquitination Assay

Cells were transfected with pcDNA-3.1-FLAG (Control) and pcDNA-3.1-FLAG-FBXO16 (FLAG-FBXO16) constructs for performing the endogenous ubiquitination assay. Cells were treated with 10 μM proteasomal inhibitor MG132 drug (Sigma, Cat #474787) for 6 h before harvesting. Nuclear fractions were immunoprecipitated with β-catenin antibody and probed using ubiquitin antibody.

Wound Healing Assay

The assay was performed using the same protocol as described earlier [24]. Wound healing capabilities were measured using Image J software.

Topflash/Fopflash Reporter Assay

Cells were seeded in a 6-well plate and cultured until confluency. Cells were transfected with either 2 μg of TOPFlash (TCF/LEF Reporter Plasmid) or FOPFlash (mutant, inactive TCF/LEF binding site) plasmids using either FBXO16 or control plasmids. Luciferase activities were measured using Dual-Luciferase Reporter (DLR) assay system following manufacturer's instructions (Promega, Wisconsin USA).

Tumorigenicity Assay

The animal studies were approved by the Institutional Animal Ethics Committee (IAEC) of NCCS. For *in vivo* tumorigenicity assays, 1×10^6 of FLAG-control and FLAG-FBXO16-RANG-2 cells were injected subcutaneously into NOD-SCID mice. Tumor volumes were determined using the formula: 4/3 Π (major axis/2^2 × minor axis/2) over a 15 days period and tumor weight was measured using weighing balance.

Statistical Analyses

Data presented here represents: mean +/-SD or mean +/-SEM from at least 3 independent experiments. Statistical analysis was performed using a 1-way ANOVA followed by either Student's t-test or Fisher's exact test. Differences between groups were statistically significant at $^*P \le .05$; $^{**}P \le .01$; $^{***}P \le .001$. Graphs were plotted using Sigma Plot 11.

Results

Expression of FBXO16 is Downregulated in GBM tumors

Previously, we have reported development of several model systems to study tumor progression in GBM [25,26]. Here, we describe generation of a yet another model system comprising of two sequentially developed long-term cultures RANG-1 and RANG-2 from a recurrent glioblastoma tumor tissue. Till p14, the RANG-1 culture showed the presence of flat, elongated neuronal-like cells (Figure 1*A*). However, at p15 several spontaneously immortalized clones dominated the plate. These spontaneously immortalized clones comprised of individual cells that were small, refractive and exhibited rapid proliferation (Figure 1*B*). Amongst the various developed clones, we chose two clones from RANG-1 and expanded them into continuously proliferating cell lines RANG-2 and RANG-3. These two immortalized cell lines showed greater than 4 folds increase in cell proliferation (Figure 1*C*) as compared to RANG-1 cell line. Considering similar growth attributes of the two cell lines, RANG-2 and RANG-3 and to avoid repeatability, we are here presenting data of only one cell line i.e. RANG-2. In line with the MTT assay, the RANG-2 cells showed intense positivity for Ki67 expression (Figure 1*D*, *E*). Interestingly, the RANG-2 cells showed presence of stem cell features like the ability to form neurospheres under serum-free condition (Figure 1*F*), positivity for expression of stem cell markers like CD133 and SOX2 (Figure 1*G*) and high migratory potential in scratch assay (Figure 1*H-I*). In contrast, the RANG-1 cells were devoid of neuropshere and tumor forming potential, did not express any of the stem cell markers like CD133 and SOX2 and expressed GFAP (Supplementary Figure 1*A*). More importantly, the RANG-2 cells formed tumors of size of about $800mm^3$ +/− 71.6 (mean volume +/− SEM) in NOD-SCID mice within 15 days of injection (Figure 1*J-K*) highlighting the tumorigenic potential of RANG-2 cell line.

Next, we mined data from Rembrandt database for expression of FBXO16 in glioma tumor tissues to determine whether there was any correlation between its expression and patient survival. Kaplan-Meir survival curve indicated that glioma patients with lower levels of FBXO16 survived for 10 years and 9 months, whereas patients with higher FBXO16 levels survived beyond 20 years (Figure 1*L*). This implied that FBXO16 was important for increasing patient survival and hence we determined levels of FBXO16 at the mRNA level in glioma tumor tissues and compared these levels to that of normal brain by qRT-PCR. A distinct downregulation in levels of FBXO16 was seen in GBM tumor tissues (n = 11) as compared to normal brain tissues (mean, n = 4) ($P \le .001$) (Figure 1*M*). Further analyses at the protein level using Western blotting indicated downregulation of FBXO16 in RANG-2 cells (Figure 1*N*). Interestingly, a similar pattern of expression was evident in clinical specimens of glioma tumor tissues, wherein using immunohistochemical analysis we found nuclear positivity for FBXO16 expression in low-grade gliomas but a weaker expression in high-grade gliomas (Figure 1*O* and Supplementary Figure 1*B*). In conclusion, a strong downregulation of FBXO16 occurs in high-grade glioma (HGG) suggesting its tumor suppressive role in GBM.

Aberrant Wnt Signaling Pathway in RANG-2 Cells

To determine whether lowered expression of FBXO16 was related to an activated Wnt signaling in RANG-2 cells, we evaluated expression of β-catenin in a panel of patient-derived glioblastoma cell lines. We found an inverse correlation between levels of FBXO16 protein to that of β-catenin in these cell lines (Figure 2*A*). The RANG-2 cell line demonstrated least level of FBXO16 but showed highest amount of β-catenin (Figure 2*A*). This reciprocity in levels was also evident in knockdown experiments wherein decrease in FBXO16 levels caused increase in β-catenin levels (Figure 2*B*). In a parallel experiment, wherein we overexpressed FBXO16 in GBM cell

lines, there was a concomitant decrease in β-catenin levels in each of them (Figure 2*C*). Importantly, the β-catenin expression observed in RANG-2 cells (highly tumorigenic) was predominantly nuclear indicating an activated Wnt signaling in these cells. Levels of nuclear β-catenin got significantly diminished upon ectopic expression of FBXO16 (Figure 2*D-E*). The non-tumorigenic RANG-1 and HEK293T showed a pre-dominant membranous staining for β-catenin as compared to highly tumorigenic cell lines RANG-2, NSG-K16 and HNGC-2 that showed high accumulation of β-catenin in their nucleus (Supplementary Figure 2). Ectopic expression of FLAG-FBXO16 construct caused dose-dependent downregulation of β-catenin in RANG-2 cells followed by a concomitant decrease in levels of β-catenin downstream target genes like Cyclin D1 [27] and c-Myc [28] (Figure 2*F*). These downstream target genes are transcriptionally activated as a result of LEF1/TCF4 interaction with β-catenin [29]. We also determined whether the LEF1/TCF4 mediated transcriptional inhibition resulted due to downregulation of β-catenin and was an outcome of FBXO16 overexpression. Hence, an immunoprecipitation assay was performed in RANG-2 cells to analyze interaction of LEF1 with β-catenin. Expectedly, under conditions of low FBXO16 expression, more β-catenin was bound to LEF1 in contrast to cells that had higher levels of FBXO16 (Figure 2*G*). Similarly, a significantly attenuated TOPFlash luciferase promoter (containing TCF/LEF binding sites for β-catenin) activity was seen in GBM cells upon FBXO16 overexpression (Figure 2*H*). Collectively, these results establish β-catenin as a novel interactor of FBXO16 and further demonstrate that its nuclear accumulation is an outcome of donwregulated FBXO16 in GBM.

FBXO16 Proteasomally Degrades β-catenin Independent of GSK-3β

There were no changes in levels of β-catenin upon FBXO16 overexpression in the RANG-2 cells at the transcriptional level (Figure 3*A*). The cytoplasmic pool of β-catenin is tightly regulated via phosphorylation by the 'destruction complex' in the absence of Wnt signaling [30]. Hence, we sought to investigate the mechanism of β-catenin destruction mediated through FBXO16 in RANG-2 cells. We transfected RANG-2 cells with FBXO16 followed by MG132 treatment and compared the expression of β-catenin with the untransfected control cells. Here, the control RANG-2 cells showed high expression of β-catenin, which was substantially decreased upon FBXO16 overexpression (Figure 3*B-C*). Instead with MG132, the FBXO16 overexpressing cells showed stabilization of β-catenin indicating that its degradation occurred through the proteasome pathway. Since, the FBOX family of proteins mediate their function by interacting with substrate proteins, we analyzed whether β-catenin was one of the interacting protein partners for FBXO16. An immunoprecipitation assay demonstrated a robust interaction of FBXO16 with β-catenin in both RANG-2 and LN229 cell lines (Figure 3*D*). Subsequently, this interaction was responsible for β-catenin degradation as FBXO16 overexpression prevented β-catenin accumulation in the nucleus of transformed cells.

The GSK-3β kinase is involved in phosphorylation of β-catenin at Serine 33, Serine 37 and Threonine 41 residues and the phosphorylated β-catenin is targeted for ubiquitination followed by degradation by β-TrCP1 [31]. To determine whether FBXO16 mediated degradation of β-catenin was GSK-3β dependent, we treated RANG-2 cells with GSK-3β inhibitor BIO (5 mM) [32]. Here, we found that cells treated with BIO showed significant reduction in β-catenin expression in FBXO16 overexpressing RANG-2 cells (Figure 3*E-F*). In a parallel experiment, RANG-2 cells were treated with another GSK-3β inhibitor, LiCl and a similar decrease in β-catenin expression was obtained in FBXO16 overexpressing cells (Figure 3*G-H*). These experiments confirmed that FBXO16 mediated degradation of β-catenin was GSK-3β independent. Next, we used a deletion mutant of RFP-β-catenin that lacked all the three GSK-3β phosphorylation sites at the Serine 33, Serine 37 and Threonine 41 residues and co-transfected it along with FLAG-FBXO16 construct in HNGC-2 (Figure 3*I*) and RANG-2 (Figure 3*J*) cell lines. We found that cells overexpressing RFP-β-catenin co-transfected with FBXO16 construct showed decreased β-catenin expression as compared to control vector co-transfected cells. These results establish a specific role of FBXO16 in proteasome-mediated degradation of β-catenin that is independent of GSK-3β.

FBXO16 Restrains Tumorigenic Potential by Degrading Nuclear β-catenin

The differential localization of β-catenin either to the nucleus, cytoplasm or to the cell membrane is a major determinant of Wnt activity [33]. Hence, to determine the fraction of β-catenin undergoing degradation, we performed subcellular fractionation assay. Overexpression of FBXO16 caused a substantial decrease in nuclear β-catenin, whereas the cytoplasmic β-catenin levels remained unchanged. This indicated that FBXO16 was selectively involved in degradation of nuclear β-catenin (Figure 4*A*). Similar findings were reiterated by confocal microscopy in RANG-2 cells co-transfected with FBXO16 and RFP-β-catenin constructs, wherein we found 4 fold reduction in accumulation of RFP-β-catenin speckles in the nucleus of FBXO16 overexpressing cells as compared to control cells (Figure 4*B-C*). A specific interaction of FBXO16 with nuclear β-catenin in RANG-2 cells was confirmed by the IP assay (Figure 4*D*). For this, the nuclear lysate proteins from the EV and FBXO16 overexpressing cells were immunoprecipitated with β-catenin and immunoblotted with K48-linked antibody. Being a component of E3 ligase, FBXO16 overexpression also enhanced ubiquitination of nuclear β-catenin and K48-linked poly-ubiquitination of β-catenin (Figure 4*E-F*). Importantly, FBXO16 regulated proteasome mediated degradation of the nuclear pool of β-catenin. The effects of β-catenin on cellular proliferation and metastasis are mediated through its various downstream target proteins like Cyclin D1, c-Myc and matrix metalloproteinases [34–36]. The FBXO16 overexpressing cells showed weaker expression of Ki67 (Figure 4*G*) and a significantly reduced migration of about 30% ($P \leq .008$) as compared to control cells indicating tumor suppressive effect of FBXO16 (Figure 4*H, I*). More importantly, the cells upon FBXO16 overexpression exhibited significantly reduced tumors as compared with control cells (Figure 4*J* and Supplementary Figure 4*A & B*). Collectively, these results establish role of FBXO16 as a tumor suppressor in GBM.

C-Terminal of FBXO16 Interacts With β-Catenin And Mediates Its Degradation

To map the region of FBXO16 that was responsible for interacting with β-catenin, we used several deletion mutants of FBXO16 protein. Besides the full-length (292 aa) FBXO16 protein, we used three FBXO16 deletion mutants corresponding to deletions at the N-terminus (1 to 85aa), F box (86 to 132aa) and C-terminal (133 to 292aa) (Figure 5*A*) regions of the FBXO16 protein and performed IP

studies. The nuclear fraction of cells overexpressing these deletion mutants were immunoprecipitated with the FLAG antibody and probed with β-catenin. We found that the C-terminal deletion mutant of FBXO16 completely lost its interaction with β-catenin, whereas cells transfected with F-box and N-terminal deletion mutants were able to interact with β-catenin (Figure 5*B*). We also performed a

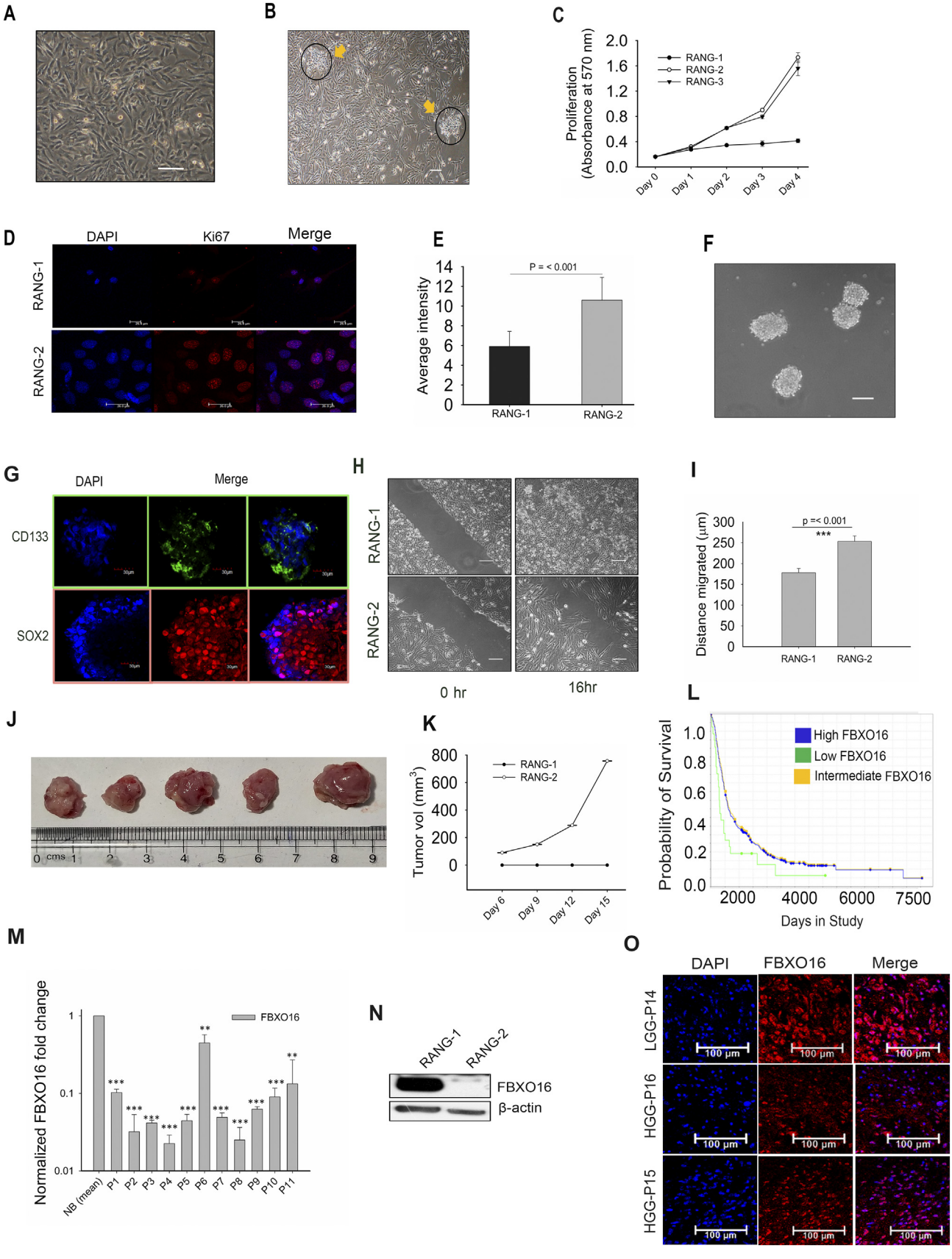

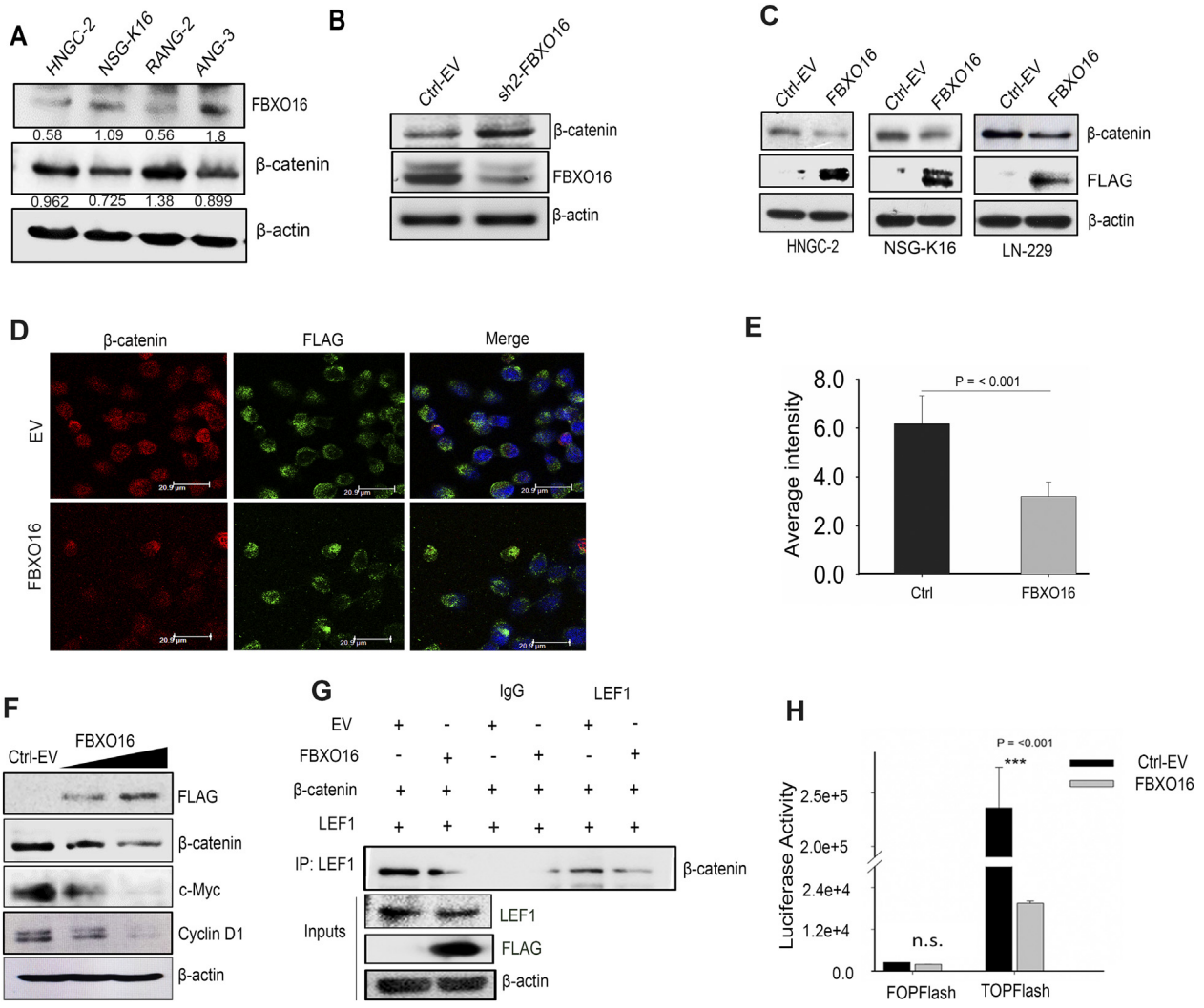

Figure 2. FBXO16 regulates β-catenin and its target genes in glioblastoma. (A) Protein levels of FBXO16 and β-catenin in patient derived GBM cell lines. β-actin serves as loading control. (B) β-catenin expression in RANG-2 cells transiently transfected with control and pLKO-FBXO16 sh2RNA. (C) Expression of β-catenin upon overexpression with FLAG-FBXO16, FLAG serves as transfection control and β-actin serves as loading control. (D) Confocal imaging and its quantitation for β-catenin in FLAG-FBXO16 overexpressing RANG-2 cells. Expression of β-catenin and FLAG-tagged FBXO16 was visualized using Alexa-594 (red) and Alexa-488 (green) secondary antibodies and counterstained with DAPI. (E) β-catenin expression quantitated with densitometry, data represented as mean +/-SD, $P \leq .001$. (F) RANG-2 cells were transfected with FBXO16 construct (0, 3 μg and 6 μg) and analyzed for expression of β-catenin, c-Myc and Cyclin D1 by Western blotting. β-actin serves as loading control. (G) IP showing interaction of LEF1 with β-catenin. The inputs for IP LEF1, FLAG and β-actin are shown in lower panel. (H) Super 8×TOPFlash luciferase promoter assay in RANG-2 cells overexpressing FBXO16 construct. The bar graph represents luciferase activity in cells transfected with FBXO16 construct. Cells transfected with pcDNA3.1 served as control. Values represent mean +/− SD (n = 3); $P \leq .001$.

Super 8×TOPFlash luciferase promoter assay with each of the deletion mutants of FBXO16 and compared the luciferase activity of the mutants to that with the full-length FBXO16. Interestingly, we found that the N-terminal deleted FBXO16 significantly showed lower luciferase activity as compared to the C-terminal and F-box domain deleted mutants (Figure 5*C*). This data indicated that the C-

Figure 1. FBXO16 is downregulated in patient derived glioblastoma cell lines. (A) Phase contrast micrograph of RANG-1 cells at p2, Scale bar: 25 μm. (B) Image of a spontaneously immortalized clone at p15 of RANG-1 cell line, Scale bar: 25 μm (C) MTT (proliferation assay) of two spontaneously transformed clones (RANG-2 RANG-3) compared with RANG-1. Data represented as mean (n = 3) +/− SD. (D&E) Confocal imaging of Ki67 expression in RANG-1 and RANG-2 cells and their quantification. (F) Neurosphere assay at 10×, Scale bar: 125 μm. (G) Confocal imaging of neurospheres for expression of CD133 and SOX2 at 60× magnification Scale bar: 30 μm. (H&I) Migration assay and its quantification at 0 h and 20 h in RANG-1 and RANG-2 cells, Scale bar: 50 μm. Data represents mean +/− SD (n = 3); $P \leq .001$. (J) Tumorigenicity assay in NOD-SCID mice with RANG-2 cells. (K) Tumor kinetics of RANG-1 and RANG-2 cells injected subcutaneously in NOD-SCID mice. Data represented as mean (n = 5) +/− SEM. (L) Kaplan–Meier curve showing survival in days of glioma patients classified on the basis of their FBXO16 levels using the Rembrandt Database. (M) qRT-PCR analysis for FBXO16 expression in glioma patients of various grades (n = 11). The FBXO16 expression was normalized to that of normal brain (n = 4). 18S rRNA served as an internal control. (N) Western blotting showing FBXO16 levels in patient derived glioma cell lines. β-actin serves as loading control. (O) Immunohistochemistry analysis of FBXO16 expression in patients representative of LGG, Gliosarcoma and Glioblastoma tumors. Scale bar: 100 μm.

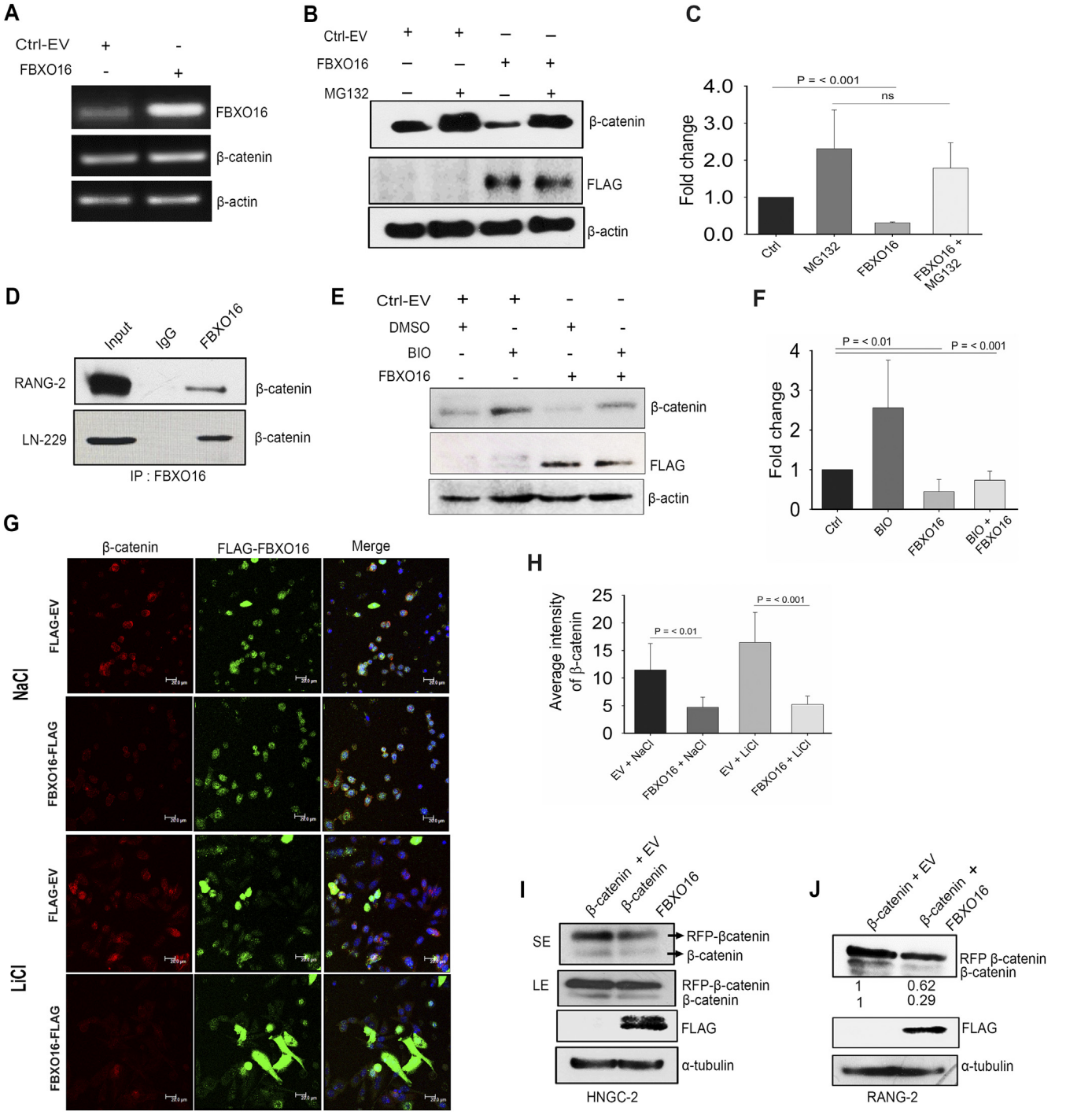

Figure 3. FBXO16 mediates proteasomal degradation of β-catenin. (A) RT-PCR analyses for expression of β-catenin. β-actin served as loading control. (B) Expression of β-catenin in cells treated with MG132. (C) Quantification of protien levels of β-catenin. Data represents mean +/− SD (n = 3); $P \leq .001$ (D) IP showing interaction of FBXO16 with β-catenin in whole cell lysates in RANG-2 and LN-229 cells. (E) Western blotting for β-catenin in cells treated with 5 μM of GSK-3β inhibitor BIO in Control and FLAG-FBXO16 transfected RANG-2 cells. (F) Quantification of protein levels of β-catenin. Data represents mean +/− SD; $P \leq .01$ & $P \leq .001$ (G&H) Confocal imaging for expression of β-catenin and its quantification in FLAG-FBXO16 or control-EV transfected RANG-2 cells. Cells were treated either with 20 mM of NaCl or LiCl solution (20 mM). Expression of β-catenin and FLAG-tagged FBXO16 was visualized using Alexa-594 (red) and Alexa-488 (green) secondary antibodies and counterstained with DAPI. Quantification data represents mean +/− SD; $P \leq .01$ and $P \leq .001$ (I) β-catenin expression in cells, co-transfected with FBXO16 and RFP–β-catenin deletion mutant (ΔS33, ΔS37, ΔT43) in HNGC-2 cells. (J) β-catenin expression in cells co-transfected with FBXO16 and RFP–β-catenin deletion mutant (ΔS33, ΔS37, ΔT43) in RANG-2 cells.

terminal region of FBXO16 was required for interaction with β-catenin. Furthermore, we analyzed the effect of each of these mutants on β-catenin levels. Interestingly, it was only the N-terminal deleted cells that had lower levels of β-catenin. This specified that the N-terminal of FBXO16 was not involved in degradation of β-catenin but in the ubiquitination of β-catenin; whereas the C-terminal region was important for interaction with β-catenin. Therefore, levels of β-catenin were unaffected by overexpression of C-terminal and F-box

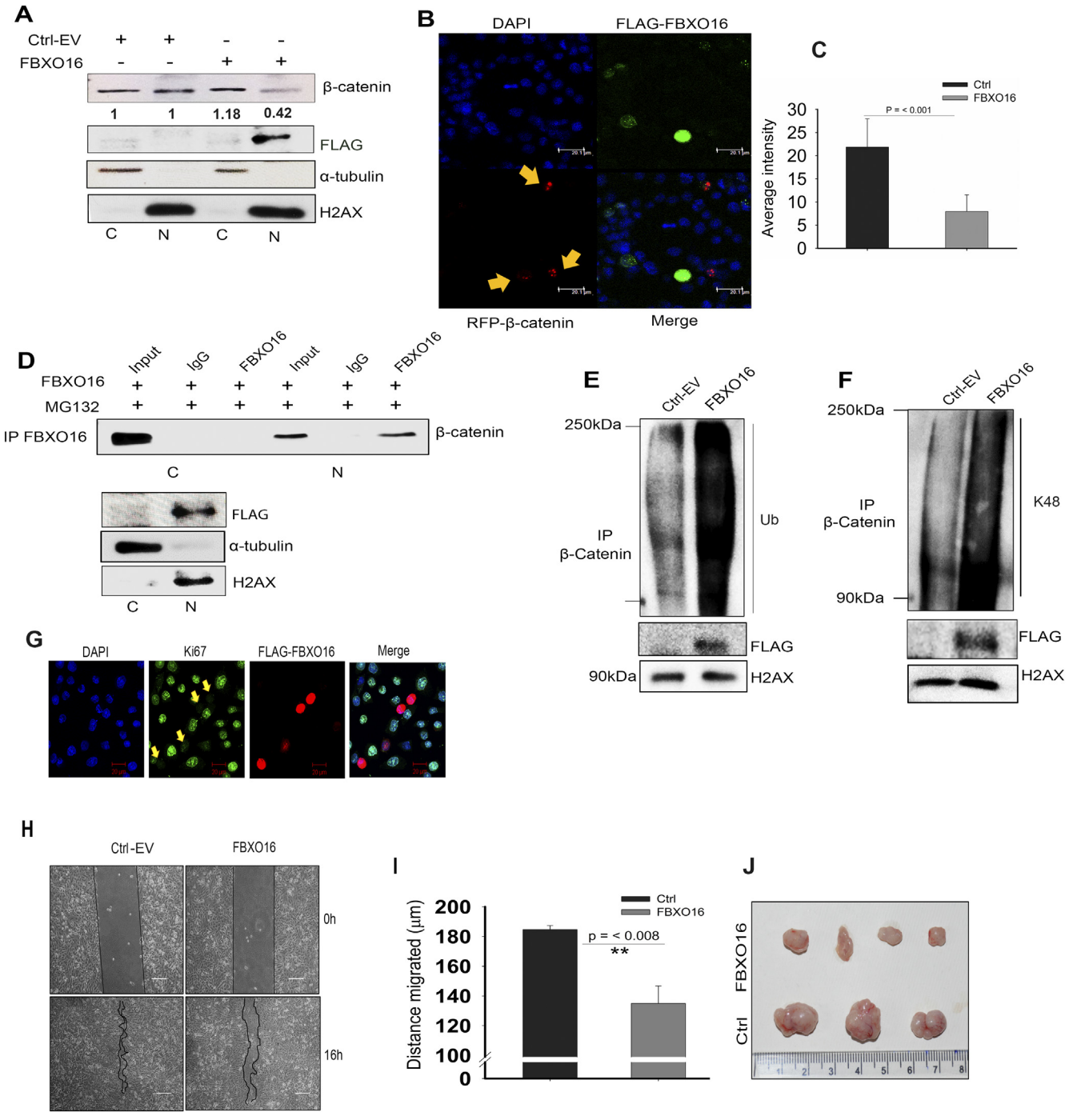

Figure 4. FBXO16 proteasomally degrades nuclear β-catenin and functions as tumor suppressor. (A) β-catenin level in cytoplasmic vs nuclear fractions of control and FLAG-FBXO16 transfected RANG-2 cells. α-tubulin served as cytoplasmic control and H2AX served as nuclear control in subcellular-fractionation. (B) Confocal imaging for β-catenin in RANG-2 cells co-transfected with RFP–β-catenin (Δ S33, Δ S37, Δ T43) and FLAG-FBXO16. Expression of FLAG-tagged FBXO16 was visualized using Alexa-488 (green) secondary antibody; RFP-labeled β-catenin was visualized at 594 wavelength and counterstained with DAPI. (C) Quantification data represents mean +/− SD; $P \leq .001$. (D) Immunoprecipitation assay showing interaction of FBXO16 with β-catenin in cytoplasmic vs nuclear fractions. α-tubulin and H2AX serve as controls. IP showing (E) poly-ubiquitination and (F) K48-linked polyubiquitination of nuclear β-catenin, in RANG-2 cells transfected with control vector or FBXO16 construct. (G) Confocal staining of Ki67 in FBXO16 overexpressing RANG-2 cells. Expression of Ki67and FLAG-tagged FBXO16 was visualized using Alexa-594 (red) and Alexa-488 (green) secondary antibodies and counterstained with DAPI. 60× magnification, Scale bar: 20 μm. (H) Cell migration assay in RANG-2 cells transfected with control vector or FBXO16 construct at 4× magnification, Scale bar: 50 μm. (I) Quantification of cell migration, data as mean +/− SD (n = 3); $P \leq .008$ (J) Subcutaneous tumors in SCID mice with control vector and FLAG-FBXO16-RANG-2 cells.

deletion constructs (Figure 5*D*). Similar findings were represented in confocal staining of β-catenin expression in cells transfected with the deletion mutants of FBXO16, wherein we observed that the N-terminal deletion mutant of FBXO16 showed significantly down-regulated β-catenin staining in the nucleus as compared to the C-terminal and F-box deletion mutants (Figure 5*E*). A schematic

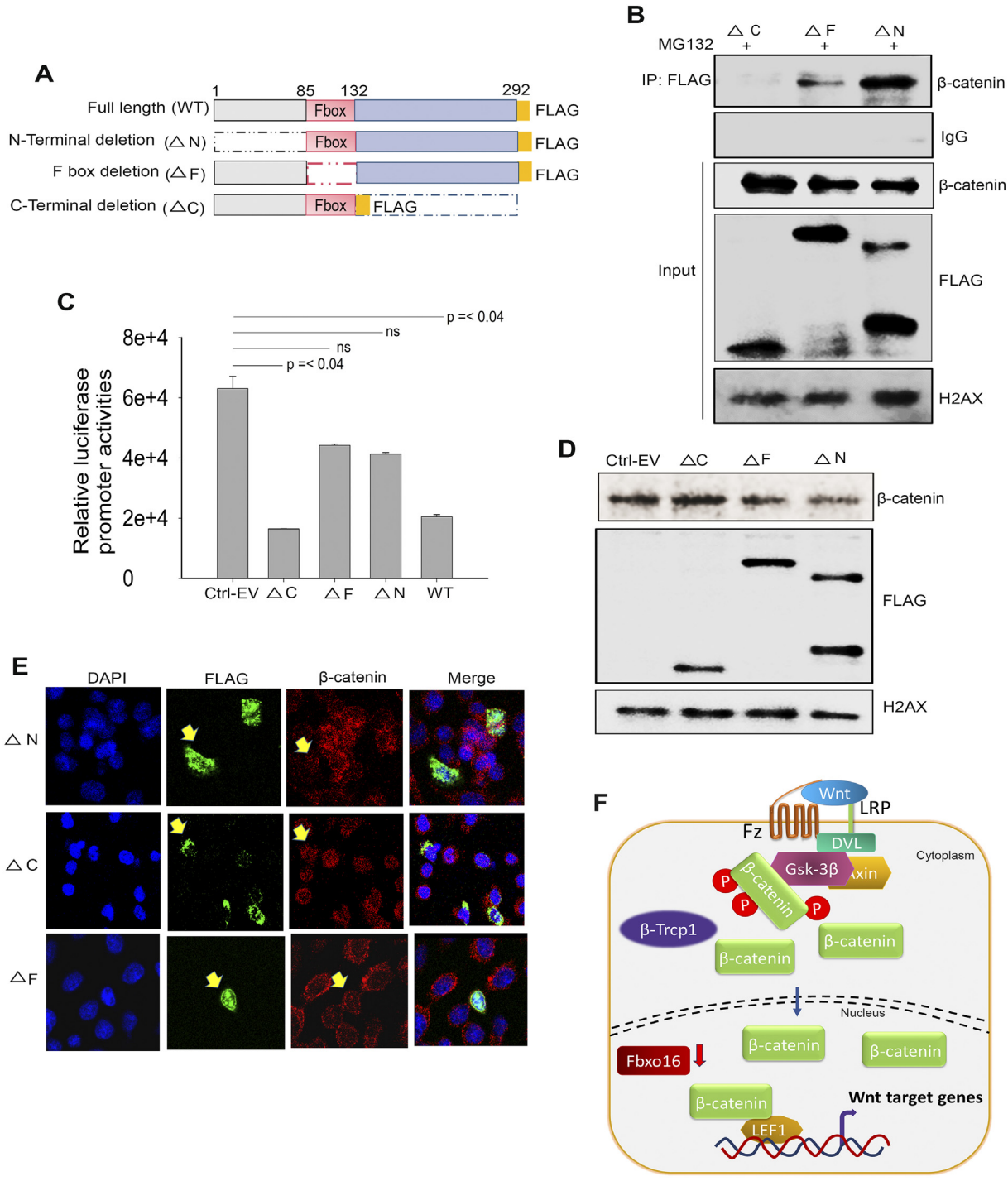

Figure 5. Interacting region of FBXO16 with β-catenin. (A) Schematic representation of deletion mutants for N-terminal, C-terminal and F-Box region along with full length FBXO16 gene. (B) IP of individual FBXO16 deletion mutants and β-catenin in nuclear fractions. (C) Super 8× TOPFlash luciferase promoter activities in RANG-2 FBXO16 (WT) compared with RANG-2-deletion mutant cells, Data represents as mean +/− SD (n = 3); $P \leq .001$ (D) RANG-2-FBXO16 deletion mutants analyzed for β-catenin using Western blotting. H2AX served as loading control. (E) Confocal imaging for β-catenin in RANG-2-FBXO16-FLAG deletion mutants. β-catenin was visualized using Alexa-594 (red) and FLAG-tagged FBXO16 mutant's staining was visualized using Alexa-488 (green) secondary antibodies and counterstained with DAPI. (F) Schematic representation of the mechanism of β-catenin stabilization in glioblastoma.

representation of β-catenin stabilization in the context of tumor suppressive role of FBXO16 in GBM is represented in Figure 5*F*. Collectively, these results indicate that the F-box domain is involved in the ubiquitination whereas the C-terminal region is required for its interaction with β-catenin.

Discussion

GBM inadvertently suffers from high levels of intra-tumoral heterogeneity. The cell line RANG-1 developed by us from a recurrent glioblastoma tumor tissue contains a mixed population of cells with varying growth potential. RANG-1 cells upon continuous

passaging (p15) showed development of several spontaneously immortalized clones. We chose two clones and established long term cell lines from them and termed them as RANG-2 and RANG-3 cell lines respectively. These cell lines consisted of small, refractive cells that were highly tumorigenic as they were able to successfully engraft in the mouse subcutaneously. In the present study, we analyzed differences between the spontaneously immortalized cells like RANG-2, RANG-3 with pre-malignant cells like RANG-1 and thereby determined mechanisms that contribute to their malignant potential. In line with our previous studies, wherein we had documented role of activated Wnt signaling in glioma progression [37], we here proceeded to investigate whether there was specific activation of β-catenin mediated Wnt pathway in RANG-2 cells. We observed a specific enrichment of β-catenin in the nucleus of RANG-2 cells demonstrating that an activated Wnt signaling was responsible for development of its highly malignant state. Besides RANG-2 cells, nuclear localization of β-catenin was also evident in other high-grade glioma cell lines like in the HNGC-2 and NSG-K16 cell-lines as well. Cytoplasmic level of β-catenin is tightly regulated via its phosphorylation by the 'destruction complex' consisting of APC, AXIN and GSK-3β [38]. β-TrCP1, a member of the FBXW family is known to degrade the phosphorylated β-catenin by ubiquitin-proteasome pathway in cytoplasm [39]. Lower levels of β-TrCP protein in glioma cells as compared to normal brain is associated with poor survival in patients with glioma [40]. However, the affinity of β-TrCP1 for β catenin is very low. This suggests that there could also be other members of the E3 ubiquitin ligase family that may be involved in degradation of nuclear β-catenin. In a search to determine whether other members of F-box family proteins might also be involved in degradation of nuclear β-catenin, we hit upon a hereto unidentified member of the FBXO family, FBXO16 as a novel interactor of β-catenin. Here, we show that FBXO16 is causal for targeting β-catenin for degradation and maintaining Wnt signaling in an Off State. We also report a tumor suppressive role for FBXO16 in GBM. The various proteins of the FBXO family are known to exert either an oncogenic or tumor suppressive function, depending on whether the deregulated degradation was occurring for oncoproteins or tumor suppressors by SCF E3 ubiquitin ligases [41]. Out of 36 well-characterized FBOX proteins, many were shown to be downregulated in various cancers like FBXO1 in hepatocellular carcinomas. Mice with homozygous FBXO1 deletion were found to be embryonically lethal and showed developmental abnormalities. Multiple reports have indicated role of various members of FBXO family in degradation of several substrates leading to tumorigenesis. To name a few are Cyclin B1 for FBXO1, Cyclin D1 for FBXO4 and HURP a cell cycle regulated oncogene for FBXO7. However, there are no reports regarding functional characterization of FBXO16 in cancer except a cytogenetic study in human BRCA2-mutated breast cancer xenografts, where a loss of 8p21.1 chromosome loci is reported [42]. To date, this is one of our initial reports for functional annotation of FBXO16 in GBM pathogenesis. In summary, our results indicate that activation of Wnt signaling mediated through failure of β-catenin degradation occurring through its interaction with FBXO16 is a pivotal mechanism of oncogenesis in GBM.

Conclusions

Amongst the various FBXO proteins identified in cancer, we conclusively show that FBXO16 functions as a tumor suppressor in GBM. The growth suppression is mediated by the degradation of nuclear β-catenin by a novel FBOX protein, FBXO16. We show that the C-terminal region of FBXO16 is important for interaction specifically with nuclear β-catenin and its degradation. Lower FBXO16 expression is associated with poorer prognosis in malignant glioma patients, suggesting that strategies aiming at restoring FBXO16 levels could open up new vistas in GBM therapy.

Supplementary data to this article can be found online at https://doi.org/10.1016/j.neo.2018.11.005.

Conflict of interest statement

The authors declare no Conflict of Interest.

Acknowledgements

We thank Jomon Joseph (JJ) and Manas Santra (MS) from NCCS, Pune, India for providing us with RFP-β-catenin and His-ub plasmids.

References

[1] Cloughesy TF, Cavenee WK, and Mischel PS (2014). Glioblastoma: from molecular pathology to targeted treatment. *Annu Rev Pathol* **9**, 1–25.
[2] Holland EC (2000). Glioblastoma multiforme: The terminator. *Proc Natl Acad Sci U S A* **97**, 6242–6244.
[3] Lathia JD, Mack SC, Mulkearns-Hubert EE, Valentim CL, and Rich JN (2015). Cancer stem cells in glioblastoma. *Genes Dev* **29**, 1203–1217.
[4] Yan H, Parsons DW, Jin G, McLendon R, Rasheed BA, Yuan W, Kos I, Batinic-Haberle I, Jones S, and Riggins GJ, et al (2009). IDH1 and IDH2 mutations in gliomas. *N Engl J Med* **360**, 765–773.
[5] Shiraishi S, Tada K, Nakamura H, Makino K, Kochi M, Saya H, Kuratsu J, and Ushio Y (2002). Influence of p53 mutations on prognosis of patients with glioblastoma. *Cancer* **95**, 249–257.
[6] Zhao J, Ma W, and Zhao H (2014). Loss of heterozygosity 1p/19q and survival in glioma: a meta-analysis. *Neuro Oncol* **16**, 103–112.
[7] Rajbhandari R, McFarland BC, Patel A, Gerigk M, Gray GK, Fehling SC, Bredel M, Berbari NF, Kim H, and Marks MP, et al (2015). Loss of tumor suppressive microRNA-31 enhances TRADD/NF-κB signaling in glioblastoma. *Oncotarget* **6**, 17805–17816.
[8] Zhang B, Pan X, Cobb GP, and Anderson TA (2007). microRNAs as oncogenes and tumor suppressors. *Dev Biol* **302**, 1–12.
[9] Li X, Wu C, Chen N, Gu H, Yen A, Cao L, Wang E, and Wang L (2016). PI3K/Akt/mTOR signaling pathway and targeted therapy for glioblastoma. *Oncotarget* **7**, 33440–33450.
[10] Saito N, Fu J, Zheng S, Yao J, Wang S, Liu DD, Yuan Y, Sulman EP, Lang FF, and Colman H, et al (2014). A high Notch pathway activation predicts response to γ secretase inhibitors in proneural subtype of glioma tumor initiating cells. *Stem Cells* **32**, 301–312.
[11] Clement V, Sanchez P, de Tribolet N, Radovanovic I, and Ruiz i Altaba A (2007). HEDGEHOG-GLI1 signaling regulates human glioma growth, cancer stem cell self-renewal, and tumorigenicity. *Curr Biol* **17**, 165–172.
[12] Kaur N, Chettiar S, Rathod S, Rath P, Muzumdar D, Shaikh ML, and Shiras A (2013). Wnt3a mediated activation of Wnt/beta-catenin signaling promotes tumor progression in glioblastoma. *Mol Cell Neurosci* **54**, 44–57.
[13] Wu G, Xu G, Schulman BA, Jeffrey PD, Harper JW, and Pavletich NP (2003). Structure of a β-TrCP1-Skp1-β-catenin complex: destruction motif binding and lysine specificity of the SCFβ-TrCP1 ubiquitin ligase. *Mol Cell* **11**, 1445–1456.
[14] Lee Y, Lee J-K, Ahn SH, Lee J, and Nam D-H (2015). WNT signaling in glioblastoma and therapeutic opportunities. *Lab Invest* **96**, 137.
[15] Paul I, Bhattacharya S, Chatterjee A, and Ghosh MK (2013). Current understanding on EGFR and Wnt/β-catenin signaling in glioma and their possible crosstalk. *Genes Cancer* **4**, 427–446.
[16] Liu C, Kato Y, Zhang Z, Do VM, Yankner BA, and He X (1999). β-Trcp couples β-catenin phosphorylation-degradation and regulates Xenopus axis formation. *Proc Natl Acad Sci U S A* **96**, 6273–6278.
[17] Salic A, Lee E, Mayer L, and Kirschner MW (2000). Control of β-catenin stability: reconstitution of the cytoplasmic steps of the Wnt pathway in Xenopus egg extracts. *Mol Cell* **5**, 523–532.

[18] Louis DN, Perry A, Reifenberger G, von Deimling A, Figarella-Branger D, Cavenee WK, Ohgaki H, Wiestler OD, Kleihues P, and Ellison DW (2016). The 2016 World Health Organization Classification of Tumors of the Central Nervous System: a summary. *Acta Neuropathol* **131**, 803–820.

[19] Shiras A, Bhosale A, Shepal V, Shukla R, Baburao VS, Prabhakara K, and Shastry P (2003). A unique model system for tumor progression in GBM comprising two developed human neuro-epithelial cell lines with differential transforming potential and coexpressing neuronal and glial markers. *Neoplasia* **5**, 520–532.

[20] Rani SB, Rathod SS, Karthik S, Kaur N, Muzumdar D, and Shiras AS (2013). MiR-145 functions as a tumor-suppressive RNA by targeting Sox9 and adducin 3 in human glioma cells. *Neuro Oncol* **15**, 1302–1316.

[21] Reed SE, Staley EM, Mayginnes JP, Pintel DJ, and Tullis GE (2006). Transfection of mammalian cells using linear polyethylenimine is a simple and effective means of producing recombinant adeno-associated virus vectors. *J Virol Methods* **138**, 85–98.

[22] Panda S, Setia M, Kaur N, Shepal V, Arora V, Singh DK, Mondal A, Teli A, Tathode M, and Gajula R, et al (2018). Noncoding RNA Ginir functions as an oncogene by associating with centrosomal proteins. *PLOS Biol* **16**e2004204.

[23] Rathod SS, Rani SB, Khan M, Muzumdar D, and Shiras A (2014). Tumor suppressive miRNA-34a suppresses cell proliferation and tumor growth of glioma stem cells by targeting Akt and Wnt signaling pathways. *FEBS Open Bio* **4**, 485–495.

[24] Sharma A, Bendre A, Mondal A, Muzumdar D, Goel N, and Shiras A (2017). Angiogenic gene signature derived from subtype specific cell models segregate proneural and mesenchymal glioblastoma. *Front Oncol* **7**, 146.

[25] Shiras A, Chettiar S, Shepal V, Rajendran G, Rajendra Prasad G, and Shastry P (2007). Spontaneous transformation of human adult nontumorigenic stem cells to cancer stem cells is driven by genomic instability in a human model of glioblastoma, vol. 25; 2007.

[26] Shiras A, Bhosale A, Shepal V, Shukla R, Baburao VS, Krishnamurthy P, and Shastry P (2003). A unique model system for tumor progression in GBM comprising two developed human neuro-epithelial cell lines with differential transforming potential and coexpressing neuronal and glial markers, vol 5; 2003.

[27] Shtutman M, Zhurinsky J, Simcha I, Albanese C, D'Amico M, Pestell R, and Ben-Ze'ev A (1999). The cyclin D1 gene is a target of the beta-catenin/LEF-1 pathway. *Proc Natl Acad Sci U S A* **96**, 5522–5527.

[28] He T-C, Sparks AB, Rago C, Hermeking H, Zawel L, da Costa LT, Morin PJ, Vogelstein B, and Kinzler KW (1998). Identification of c-MYC as a target of the APC pathway. *Science* **281**, 1509–1512.

[29] Shimizu T, Kagawa T, Inoue T, Nonaka A, Takada S, Aburatani H, and Taga T (2008). Stabilized beta-catenin functions through TCF/LEF proteins and the Notch/RBP-Jkappa complex to promote proliferation and suppress differentiation of neural precursor cells. *Mol Cell Biol* **28**, 7427–7441.

[30] Stamos JL and Weis WI (2013). The β-catenin destruction complex. *Cold Spring Harb Perspect Biol* **5**, a007898.

[31] Aberle H, Bauer A, Stappert J, Kispert A, and Kemler R (1997). Beta-catenin is a target for the ubiquitin-proteasome pathway. *EMBO J* **16**, 3797–3804.

[32] McCubrey JA, Steelman LS, Bertrand FE, Davis NM, Sokolosky M, Abrams SL, Montalto G, D'Assoro AB, Libra M, and Nicoletti F, et al (2014). GSK-3 as potential target for therapeutic intervention in cancer. *Oncotarget* **5**, 2881–2911.

[33] Du W, Liu X, Fan G, Zhao X, Sun Y, Wang T, Zhao R, Wang G, Zhao C, and Zhu Y, et al (2014). From cell membrane to the nucleus: an emerging role of E-cadherin in gene transcriptional regulation. *J Cell Mol Med* **18**, 1712–1719.

[34] Syed V, Mak P, Du C, and Balaji KC (2008). β-Catenin mediates alteration in cell proliferation, motility and invasion of prostate cancer cells by differential expression of E-cadherin and protein kinase D1. *J Cell Biochem* **104**, 82–95.

[35] Xu J, Chen Y, Huo D, Khramtsov A, Khramtsova G, Zhang C, Goss KH, and Olopade OI (2016). Beta-catenin regulates c-Myc and CDKN1A expression in breast cancer cells. *Mol Carcinog* **55**, 431–439.

[36] Brabletz T, Jung A, Dag S, Hlubek F, and Kirchner T (1999). Beta-catenin regulates the expression of the matrix metalloproteinase-7 in human colorectal cancer. *Am J Pathol* **155**, 1033–1038.

[37] Kaur N, Chettiar S, Rathod S, Rath P, Muzumdar D, Shaikh ML, and Shiras A (2013). Wnt3a mediated activation of Wnt/β-catenin signaling promotes tumor progression in glioblastoma. *Mol Cell Neurosci* **54**, 44–57.

[38] Li Vivian SW, Ng Ser S, Boersema Paul J, Low Teck Y, Karthaus Wouter R, Gerlach Jan P, Mohammed S, Heck Albert JR, Maurice Madelon M, and Mahmoudi T, et al (2012). Wnt signaling through inhibition of β-catenin degradation in an intact Axin1 complex. *Cell* **149**, 1245–1256.

[39] Liu C, Kato Y, Zhang Z, Do VM, Yankner BA, and He X (1999). β-Trcp couples β-catenin phosphorylation-degradation and regulates Xenopus axis formation. *Proc Natl Acad Sci U S A* **96**, 6273.

[40] Liang JUN, Wang W-F, Xie S, Zhang X-L, Qi W-F, Zhou X-P, Hu J-X, Shi Q, and Yu R-T (2015). Expression of β-transducin repeat-containing E3 ubiquitin protein ligase in human glioma and its correlation with prognosis. *Oncol Lett* **9**, 2651–2656.

[41] Zheng N, Schulman BA, Song L, Miller JJ, Jeffrey PD, Wang P, Chu C, Koepp DM, Elledge SJ, and Pagano M, et al (2002). Structure of the Cul1-Rbx1-Skp1-F boxSkp2 SCF ubiquitin ligase complex. *Nature* **416**, 703–709.

[42] de Plater L, Laugé A, Guyader C, Poupon MF, Assayag F, de Cremoux P, Vincent-Salomon A, Stoppa-Lyonnet D, Sigal-Zafrani B, and Fontaine JJ, et al (2010). Establishment and characterisation of a new breast cancer xenograft obtained from a woman carrying a germline BRCA2 mutation. *Br J Cancer* **103**, 1192–1200.